



Cite this: *Mater. Adv.*, 2025, 6, 8051

## Elucidating the impact of fiber source on polypropylene/hemp composite performance for the automotive industry

Amber M. Hubbard, <sup>a</sup> Julia Gelfond, <sup>ab</sup> Kathryn Slavny, <sup>abc</sup> Komal Kooduvalli, <sup>ade</sup> Katie Copenhaver, <sup>a</sup> Meghan E. Lamm, <sup>a</sup> Sanjita Wasti, <sup>a</sup> Matthew Korey, <sup>af</sup> Yunqiao Pu, <sup>g</sup> Caitlyn M. Clarkson<sup>a</sup> and Umesh Marathe<sup>a</sup>

Given their high strength-to-weight ratio, there is an ever-increasing volume of plastics being used in the automotive industry as plastics aid in the charge to lightweight vehicles for improved fuel efficiency. However, these plastics are often landfilled at their end-of-life, which has given rise to the demand for sustainable materials and waste management alternatives compared to purely synthetic systems. Natural fiber composites have been explored as a viable material option to reduce the environmental impact of plastic use in automobiles while simultaneously ensuring the part performance is not sacrificed. Herein, we explored the use of hemp/polypropylene (PP) composites in which US-sourced hemp is compared to internationally sourced and industrially available hemp. There appears to be a minimal impact on the composite properties regardless of fiber sourcing, and the addition of a natural filler to the PP matrix results in up to a 367% increase in Young's modulus, 126% increase in heat deflection temperature, and comparable water uptake performance. It should be noted that the natural filler addition does increase density by up to 13% due to the higher density of natural fibers compared to the low-density PP matrix. A modified rule of mixtures calculation revealed that the composite materials produced in this study demonstrated good agreement with analytical modeling. Finally, a screening analysis was performed exploring the transportation of hemp fibers, and the results build a strong case for regionalized manufacturing of automotive parts.

Received 23rd July 2025,  
Accepted 26th September 2025

DOI: 10.1039/d5ma00798d

[rsc.li/materials-advances](http://rsc.li/materials-advances)

## Introduction

As the global demand for cost-effective and efficient vehicles increases, so does the demand for plastic usage in passenger vehicles. Given the high strength-to-weight ratio for polymers and composites, they have become an enticing means to reduce vehicle weight without sacrificing performance, particularly for non-structural applications. For example, in 2023 it has been

estimated that 10% of the average vehicle weight is comprised of polymers and composites with this number signifying a 19% increase from 2013.<sup>1</sup> The demand for fuel efficiency in modern vehicles is bolstered by the fact that even a 10% decrease in a vehicle's weight has been shown to yield a 6–8% improvement in fuel performance. This is significant considering the 283.4 million vehicles registered in 2024 in the United States (US) alone, a 2.7% increase since 2022.<sup>2–4</sup>

While polymers and composites are growing in use across the automotive industry, there is a simultaneous demand to produce composites which are more environmentally friendly than their synthetic counterparts and allow for domestic production. The replacement of synthetic fiber with natural fibers in composites has been explored worldwide, and hemp fiber composites are of particular interest in the US due to their compatibility with a broad range of climates and soil qualities. Industrial hemp fibers, derived from the hemp plant (*Cannabis sativa* L.), offer an exceptional strength-to-weight ratio, flexible growing conditions, low water usage, and rapid regrowth cycle.<sup>5</sup> For example, industrial hemp benefits from increased seed density rates to allow for taller crops (height ~5–6 m) and

<sup>a</sup> Manufacturing Science Division, Oak Ridge National Laboratory, Oak Ridge, TN 37830, USA. E-mail: hubbardam@ornl.gov

<sup>b</sup> ORISE Participant in the U.S. Department of Energy Education Collaboration at ORNL Program, 1299 Bethel Valley Rd, Oak Ridge, TN 37830, USA

<sup>c</sup> ORISE Participant in the U.S. Department of Energy Science Undergraduate Laboratory Internships Program, Oak Ridge National Laboratory, 1 Bethel Valley Rd., Oak Ridge, TN, 37830, USA

<sup>d</sup> Golisano Institute for Sustainability, Rochester Institute of Technology, 190 Lomb Memorial Drive, Rochester, NY 14623, USA

<sup>e</sup> ORISE Participant in the U.S. Department of Energy Graduate Research at ORNL Program, 1299 Bethel Valley Rd, Oak Ridge, TN 37830, USA

<sup>f</sup> Department of Mechanical, Aerospace, and Biomedical Engineering, University of Tennessee, Knoxville, TN 37996, USA

<sup>g</sup> Biosciences Division, Oak Ridge National Laboratory, Oak Ridge, TN 37830, USA



increased stalk strength, which simultaneously has the benefit of higher crop output per hectare of land usage.<sup>5</sup> It should also be noted that industrial hemp contains <0.2% THC and is grown for its end use in consumer goods such as textiles, composites, building materials, paper, cement reinforcement, *etc.*, and is not subject to the same regulations as medical-grade hemp.<sup>6–11</sup>

Though other natural fibers (*e.g.*, flax, kenaf, jute, sisal, *etc.*) have previously been explored for thermoplastic composites in literature, this study focuses on the production of a variety of hemp fiber (HF)/polypropylene (PP) composites and their viability in automotive applications. Industrial hemp fiber has a comparably high tensile strength (310–750 GPa) to other natural fibers such as flax (500–900 GPa), jute (393–773 GPa), and kenaf (282–800 GPa) as well as a fast growth rate with a vegetation period of ~100 days.<sup>12,13</sup> European markets saw a 62.4% increase in industrial hemp production from 2015 to 2019, with France being the primary European hemp producing country, but the US production of industrial hemp is not listed by the United Nations Food and Agriculture Organization (FAO) as one of the world's top producers.<sup>5,13</sup> Demonstrating the ability to create commercially applicable hemp fiber composites in the US could bolster production and establish new regional manufacturing supply chains.

A wide variety of hemp fiber thermoplastic composites have been reported in literature with fiber loadings typically from 20–40 wt%, although studies have been conducted with up to 75 wt% fiber content.<sup>5,6,8,13</sup> Hemp fiber composites have been produced with thermoplastic resins such as PP, polylactic acid, and polyethylene as well as thermosetting resins like epoxies.<sup>14–18</sup> In addition, a variety of fiber treatments including maleic anhydride grafting, alkali treatments, and silane treatments have demonstrated marked improvement in composite properties due to increased polymer/fiber interfacial adhesion.<sup>19</sup> There are, however, minimal studies exploring the impact of fiber quality from various sources on composite properties for industrial applications. This is particularly relevant as fiber quality and growing conditions are crucial in dictating final composite performance. For example, Pickering *et al.* explored the impact of growing periods on industrial hemp fibers and found the optimal growing period to be 114 days, resulting in hemp fiber with an average tensile strength of 857 MPa,<sup>20</sup> while shortening the growing period to just 99 days resulted in fiber strengths <600 MPa. The tensile strength of all natural fibers is notably varied, but tensile testing in concert with strain mapping and compositional analyses has demonstrated that higher tensile performance correlates to increasingly compact microstructures.<sup>21</sup>

This study explores the use of hemp fillers from various sources in PP composites to understand the impact of fiber sourcing on composite properties. In addition, this study demonstrates scaling of these composites to larger batch sizes for injection molding for potential use in automotive applications and couples these findings with a comparative transportation analysis to explore the energy demand and greenhouse gas emissions relating to industrial hemp fiber transportation.

## Materials and methods

### Material sourcing and composite production

PP pellets (Exxon PP3155) were sourced from Channel Prime Alliance. Maleic anhydride-grafted polypropylene (MAPP) with a weight-average molecular weight ( $M_w$ ) of ~9100 was purchased from Sigma-Aldrich in pellet form for ease of incorporation into the composites. The hemp fiber from Missouri (MO) and South Dakota (SD) were provided by the Hemp Alliance of Tennessee (HAT) *via* KonopiUS, LLC and Complete Hemp Processing, LLC, respectively, and are both the hemp strain Futura 83. The international hemp fiber (Int'l) chopped to a uniform length of 6 mm was provided by MiniFIBERS, Inc., and hemp dust (HD) from fiber processing was provided by Hemp-Wood (Fibonacci, LLC). No information could be provided regarding the strain of both the Int'l fibers and the HD. All materials were used as received, other than the MO and SD hemp fiber which was processed as detailed below.

The fibers from MO and SD were pre-processed into short, chopped fibers as described in Fig. 1. The fiber processing involved hacking the fiber stalks *via* a three-step process: a wide tooth single row comb, a wide tooth double row comb, and a fine comb. The fibers were combed until the hurd fiber was removed and the bast fiber was reasonably separated and the fiber diameters appeared visually similar to the industrially processed Int'l fibers (Fig. S1). The MO and SD fibers were then manually cut to target lengths of ~6 mm. The received HD was a waste by-product from another industry and likely contained additives that were not disclosed but were included as a particulate comparison to the higher aspect ratio fibers.

The composites were produced in a Brabender Intelli-Torque Plasticorder Torque Rheometer using a 60 cc mixing heat attachment. All composites were melt mixed at 180 °C under a rotational speed of 60 rpm; the PP (and MAPP if appropriate) was mixed for 2 minutes to ensure homogeneous melting prior to the addition of the filler material, which was mixed for an

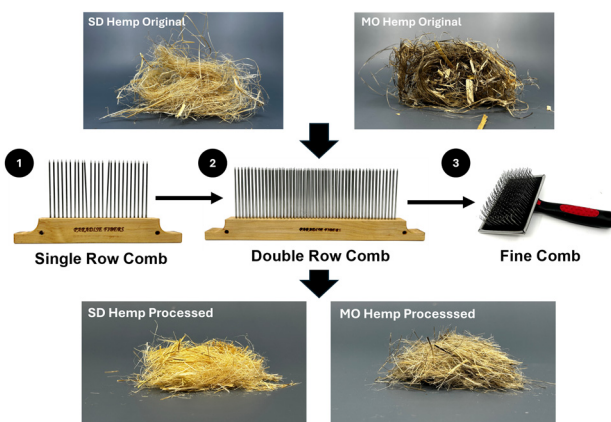


Fig. 1 A schematic diagram shows the fiber processing steps that all materials were placed through, prior to creating PP composites. The fiber processing is shown for the hemp fiber grown in Missouri (MO) and South Dakota (SD). Note that the international hemp (Int'l) and hemp dust is not shown as it did not undergo any processing once received.



additional 5 minutes. Composites were prepared at 10, 20, 30, and 40 wt% filler in PP where, unless otherwise noted, the filler concentration was 20 wt% as discussed in a later section. For composites with compatibilizer, 5 wt% MAPP was included. All materials were dried overnight at 60 °C prior to compounding. Samples were compression molded using a Carver hydraulic press at 185 °C and were held for 5 minutes under no pressure for temperature equilibration followed by ~4 metric tons of pressure for 5 minutes. The press and samples were then cooled using a circulatory chiller at 21 °C while maintaining pressure.

#### Thermogravimetric analysis (TGA)

TGA was performed on all composite materials using a TA Instruments TGA 5500 in air to investigate their thermal stability. The material was ramped from 30 °C to 600 °C at a rate of 10 °C min<sup>-1</sup>. The onset degradation temperature ( $T_{\text{onset}}$ ) and the temperature at a 2 wt% mass loss ( $T_{2\%}$ ) were recorded for all materials, as seen in Table S1 and Fig. S2.

#### Differential scanning calorimetry (DSC)

DSC was performed on all composite materials using a TA Instruments DSC 2500 instrument in an argon environment. Samples were exposed to a heat-cool-heat experiment from 0 °C to 200 °C at a temperature ramp rate of 10 °C min<sup>-1</sup>. The melting temperature ( $T_m$ ) and crystallization temperature ( $T_c$ ) were recorded for all materials (Table S1), and the crystallinity was calculated according to previously reported methods.<sup>22</sup> To ensure statistical significance, at least 3 samples were tested per material formulation.

#### Dynamic mechanical analysis (DMA)

The low stress (0.455 MPa) heat deflection temperature (HDT) was measured for all materials using a TA Instruments DMA 850 instrument in an air environment according to previously reported methods.<sup>22</sup> To ensure statistical significance, at least 3 samples were tested per material formulation.

#### Pycnometry

The density for all materials was measured using a Micromeritics AccuPyc II 1340 pycnometer in a helium environment according to a modified form of ASTM D3576. To ensure statistical significance, at least 3 samples were tested per material formulation, and 5 measurements were recorded per sample for a total of 15 measurements per formulation.

#### Water uptake

Water uptake for each sample was recorded according to a modified form of ASTM D570. Samples were submerged in DI water for at least 24 hours, and the mass increase was recorded as a function of time. To ensure statistical significance, at least 3 samples were tested per material formulation.

#### Scanning electron microscope (SEM)

The hemp fibers and dust were sputtered with platinum/palladium and imaged using a scanning electron microscope (SEM, Zeiss Merlin field emission) in secondary electron mode at an

accelerating voltage of 1 kV. In addition, the interface between the composite fiber and matrix was investigated by observing the tensile fracture surface; the fracture surfaces were sputter coated with iridium.

#### Tensile testing

Tensile properties were measured according to ASTM D3039 by stretching 120 mm × 10 mm × 3 mm ( $l \times w \times t$ ) specimens at room temperature *via* a servo-hydraulic testing machine (MTS Criterion Model 45) with a 5 kN load cell at a speed of 1.5 mm min<sup>-1</sup>. The strain on each sample was monitored using an extensometer. Five specimens for each sample were tested, and the average was reported.

#### Fiber compositional analysis

The chemical composition of the substrates was analyzed based on a modified NREL procedure.<sup>23</sup> In brief, 150 mg of biomass was loaded to 1.5 mL 72 wt% sulfuric acid and hydrolyzed at 30 °C for 1 hour. Upon completion, the mixture was diluted to 4% sulfuric acid with deionized water and further hydrolyzed at 121 °C in an autoclave for another hour. After the two-step acid hydrolysis, the solid and liquid fractions were separated by vacuum filtration. The solid fraction was dried at 105 °C overnight to gravimetrically determine the Klason lignin content. The liquid fraction was analyzed with high-performance liquid chromatography (HPLC) to determine the contents of carbohydrates (*i.e.*, glucose and xylose) using a series of glucose and xylose with varying concentrations established as a calibration curve.

#### Fourier transform infrared spectroscopy (FTIR)

FTIR was performed on all filler materials using a PerkinElmer Frontier FTIR-NIR with the ATR fixture in place. At least 16 scans were performed for each filler material across wavenumbers of 750–4000 cm<sup>-1</sup>.

#### Transportation impact assessment

A screening lifecycle assessment (LCA) was utilized to understand the greenhouse gas emissions and embodied energy associated with transporting domestic and international hemp fiber. For this purpose, global warming potential (GWP) results were obtained from the TRACI methodology<sup>24</sup> and embodied energy values from the cumulative energy demand (CED)<sup>25</sup> with processes obtained from the Ecoinvent database<sup>26,27</sup> found in the SimaPro software (v.9.6.0.1).<sup>28</sup> In this study, acquisition of seeds and other raw materials, fiber growth conditions, pre-processing, and other production steps were excluded from the system boundary across all cases with the functional unit focused on the transportation of 1 kg of hemp fiber. Essentially, this analysis was meant to address whether shipping comparably dense fibers from various source locations to the same destination had an environmental impact on the final part produced. This helped conclude whether domestically sourced fibers were indeed environmentally friendlier compared to internationally sourced fibers. Herein, the only modes of transportation considered were either roadway (*i.e.*, truck) or waterway (*i.e.*, sea freight)



where the internationally sourced fiber was chosen from a region in France (one of the largest cultivation States in the European Union) where hemp is typically grown<sup>29</sup> and three domestic states (Missouri – MO, South Dakota – SD, and Tennessee – TN); additional details related to data and modeling assumptions can be found in Tables S2–S4. The destination point was Knoxville, TN for all cases where the Tennessee sourced fibers were chosen from the farthest hemp farm location from Knoxville in the state.

## Results and discussion

### Composite formulation and characterization

As the supply chain for technical hemp fiber continues to grow in the US, it is important to understand how growth locations impact fiber performance. Hemp fibers of the same strain (Futura 83) grown in two different US locations (Missouri – MO and South Dakota – SD) were obtained and compared to a non-US-grown fiber (Int'l) and post-processing hemp dust (HD). The MO and SD hemp was received directly from growers and needed significant processing prior to composite production, in which the goal was to process the fibers to a state that was comparable to the pre-processed Int'l hemp. The fiber bundles (seen in the upper row of Fig. 1) were processed through a wide-tooth single row comb, a wide-tooth double row comb, and finally a fine-tooth comb (middle row of Fig. 1) to remove the hurd and align the fibers for manual cutting. The processed fibers can be seen in the bottom row of Fig. 1, where they were added directly into the composite after being chopped to approximately 6 mm in length.

An image of all four hemp fillers can be seen in the top row of Fig. 2, accompanied by an SEM image in the bottom row. The diameters for all three fiber types were statistically comparable with averages of approximately 100–150  $\mu\text{m}$ , as shown in Fig. S1. The HD was in the form of low aspect ratio particles with dimensions below 100  $\mu\text{m}$ .

To further elucidate differences between the filler materials, compositional analyses (*i.e.*, glucan, xylan, and lignin) were

performed as seen in Table 1. Xylan is the major carbohydrate sugar specific to hemicellulose, and glucan is the sugar of cellulose. The miscellaneous portion contains extractives, waxes, ashes, and other non-structural components in hemp fibers. The three hemp fibers presented no significant difference in hemicellulose (xylan) or lignin content when calculated with a 95% confidence level, while differences did exist in their cellulose (glucan) and miscellaneous (*i.e.*, extractives, impurities, *etc.*) content. However, the HD contained a significantly higher concentration of miscellaneous material, hemicellulose, and lignin than the fibers, with a correspondingly low cellulose content. While a definitive conclusion cannot be drawn regarding the HD composition due to the presence of unknown additives, these additives likely contribute to the high miscellaneous content, while the hemp strain(s) present in this material seemingly contain relatively higher hemicellulose and lignin fractions than those of the fiber samples. It should be noted that the high hemicellulose content in the HD composites does promote lower thermal stability, as reported in Table S1 and Fig. S2.

Natural fibers have an inherently higher density than neat PP, where the composite density will vary as a function of filler type, filler concentration, crystallinity, *etc.* (Fig. 3a). A key benefit for including natural fiber composites in vehicles is the potential lightweighting benefits over metallic components and denser composites; for example, glass fiber-filled composites exhibit substantial density increases (*e.g.*, glass fiber density: 2.55  $\text{g cm}^{-3}$ ). While the composite densities exceeded that of neat PP, they remain comparable to, or lower than, PP filled with 20 wt% glass fiber (1.04  $\text{g cm}^{-3}$ ) and are substantially below that of other common automotive plastics such as polycarbonate (1.20  $\text{g cm}^{-3}$ ) or polyvinyl chloride (1.38  $\text{g cm}^{-3}$ ).<sup>30–33</sup> Moreover, composite densities with and without MAPP have been reported in the literature ranging between 0.96 and 1.02  $\text{g cm}^{-3}$ . The composites in the present study, which include hemp fillers from various geographical locations, exhibit densities within this expected range and while the differences in density are small, all but two composite densities denoted in Fig. 3a are statistically

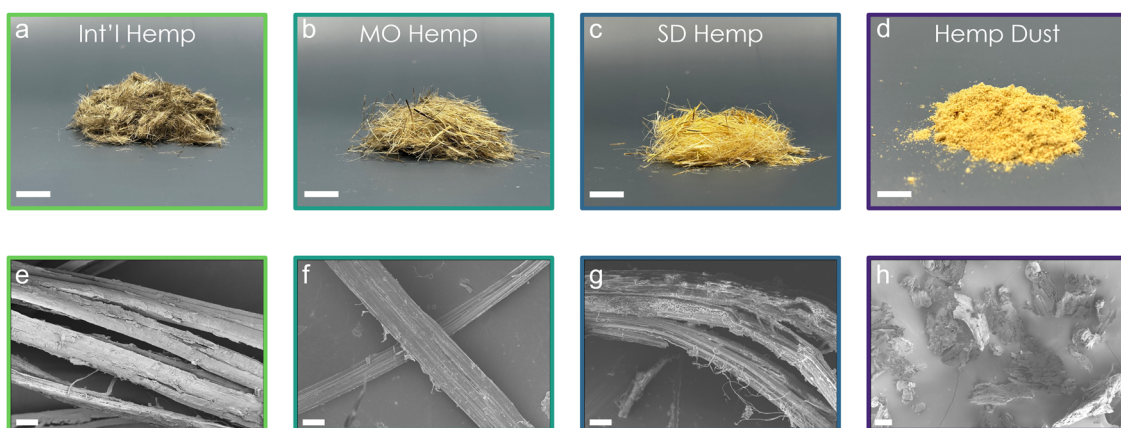
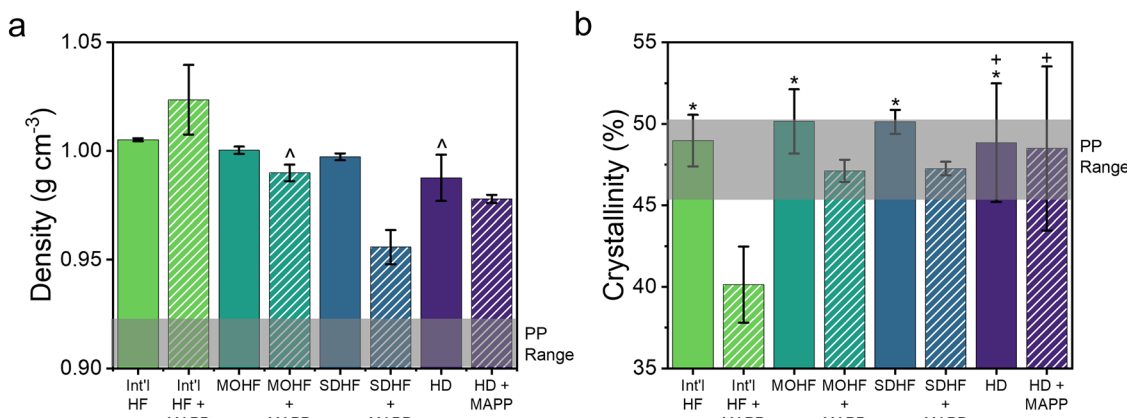


Fig. 2 Photographs and SEM images are shown for all four hemp fillers used throughout this study: (a) and (b) international hemp, (c) and (d) Missouri hemp, (e) and (f) South Dakota hemp and (g) and (h) hemp dust.



Table 1 The four hemp fillers compositional analysis is reported

Sample	Glucan (%)	Xylan (%)	Klason Lignin (%)	Miscellaneous (%)
International (Int'l) hemp fiber	78.6 ± 1.0	6.1 ± 0.5	4.1 ± 0.2	~11
Missouri (MO) hemp fiber	71.4 ± 0.0	6.9 ± 1.0	4.7 ± 0.2	~17
South Dakota (SD) hemp fiber	69.5 ± 0.6	6.7 ± 0.3	3.5 ± 0.0	~20
Hemp dust (HD)	40.5 ± 1.1	11.8 ± 0.4	15.5 ± 0.4	~32

Fig. 3 Composite properties were measured: (a) density of composites and (b) degree of crystallinity for composites. Symbols denote which samples of interest that are not statistically different ( $p > 0.05$ ) from each other: ^ MOHF + MAPP and HD; \* All neat fiber types; + HD and HD + MAPP.

different from each other. The differences in chemical composition (Table 1) between hemp types, in this case, did not significantly alter the composite density. With MAPP addition, the density decreased for composites containing MO, SD, or HD, but increased for the Int'l HF composites, as discussed in greater detail below.

Other factors that affect density include porosity or changes in the degree of crystallinity ( $X\%$ ) as crystalline polymers have a higher density than amorphous polymers.<sup>34</sup>  $X\%$  was calculated from DSC data (Fig. S2) and the results are provided in Fig. 3b. All composites with neat fibers at a 20 wt% filler concentration did not significantly affect PP crystallization nor are they significantly different from each other. It was expected that the HD might be slightly more compatible with the PP due to the higher impurity/miscellaneous content which includes inorganics like ash, however, that was not the case. The similar  $X\%$  for all hemp fiber composites is postulated to be a result of comparable compatibility of all fiber types with the PP matrix. Interestingly, the addition of MAPP, which is a compatibilizer meant to improve the matrix interaction with the more hydrophilic fillers, decreased the crystallinity of all hemp fiber composites (Fig. 3b). For example, the addition of MAPP into the Int'l, MO, and SD composites resulted in an 18%, 6%, and 6% decrease in  $X\%$ , respectively. A similar observation has been made for other natural fibers, such as sisal fiber with cellulose nanocrystals<sup>35</sup> and hemp fiber.<sup>36</sup> In contrast, other studies have reported improvements in crystallinity with the use of MAPP, such as improved dispersion and transcrystallization on highly crystalline cellulose nanofibrils.<sup>37</sup> It is postulated that the MAPP concentration plays a significant role in crystallization

of these composites. Huang *et al.*, who studied the crystallization rate of wood plastic composites based on PP and MAPP, have observed that MAPP can increase the crystallization rate but results in a lower total degree of crystallinity and that at higher MAPP contents, MAPP will hinder crystallization.<sup>38</sup> This is a possible explanation for the decrease in crystallinity for the present study as MAPP concentration was not optimized to achieve a specific crystallinity. Likewise, as noted above, a decrease in density was observed for MOHF and SDHF composites with the addition of MAPP. This is reasonable given that lower crystallinity values typically indicate lower density values; for example, the density of amorphous and crystalline PP is  $0.87\text{ g cm}^{-3}$  and  $0.92\text{--}0.939\text{ g cm}^{-3}$ , respectively.<sup>34</sup> There are two exceptions to the expected trend with density and crystallinity: (1) the HD and HD + MAPP composites decrease in density with no statistical difference in crystallinity and (2) the Int'l HF increase in density with a statistically significant decrease in crystallinity. This deviation from the expected trend might be explained by sample-to-sample variance. As to why some hemp fiber types experienced a more significant loss in crystallinity with the addition of MAPP, such as the Int'l HF which also has the highest cellulose (glucan) content, it may be that the MAPP coupled more strongly with the Int'l HF surface compared to the other fiber sources resulting in stronger hindrance of crystallization for this material. However, the expectation would be that superior coupling would result in an increase in tensile strength, which as will be discussed later, is not necessarily the case for the Int'l HF + MAPP composites.

To determine the optimum hemp filler concentration, each hemp fiber was melt compounded into the PP matrix in 10 wt%

increments from 10–40 wt%. The expected Young's modulus was calculated using a modified rule of mixtures (ROM) calculation, given in eqn (1),

$$E_c = \eta_0 E_f V_f + E_m V_m \quad (1)$$

in which  $E_c$ ,  $E_f$  and  $E_m$  represent the modulus of the composite, fiber, and matrix respectively.<sup>39</sup>  $V_f$  and  $V_m$  denote the volume fraction of the fiber and matrix, respectively, and  $V_f + V_m = 1$ . Furthermore,  $\eta_0$  represents composite efficiency factor (Krenchel) with values for unidirectional, biaxial and random (in-plane) fiber orientation of 1, 0.5 and 0.375 respectively.<sup>39</sup> The fiber volume fraction was calculated using eqn (2) below,

$$V_f = \frac{\frac{W_f}{\rho_f}}{\frac{W_f}{\rho_f} + \frac{W_m}{\rho_m}} \quad (2)$$

in which  $\rho_f$  and  $\rho_m$  represent the density of the fiber and matrix, respectively, and  $W_f$  and  $W_m$  represent the respective weight fractions of the fiber and matrix. For these calculations, the hemp fiber density was assumed to be 1.4–1.5 g cm<sup>-3</sup>, and the Young's modulus was assumed to be 30–60 GPa.<sup>12</sup> The predicted modulus values of hemp fiber composites are shown in Fig. 4 as a function of fiber content.

The range of reported modulus values in Fig. 4 is a result of the ranges used for density and modulus values and reflects the inherent variability of natural fibers. The HD was not represented on this graph, as only the fibers were considered in this calculation. There is reasonable agreement between the calculated modulus range and the experimental data, with the MO fiber composites demonstrating the strongest agreement. The theoretical values obtained from the model followed the trend of increasing modulus with the increase in fiber content. The model generally overpredicted modulus, especially in cases of higher fiber loading (30–40 wt%). At increasingly higher fiber loadings, it is difficult to achieve strong adhesion between the fiber and matrix due to inadequate wetting. This creates

microstructural defects and voids prohibiting complete utilization of the fiber's stiffness. Since the model assumes a perfect fiber-matrix adhesion along with the absence of voids and defects, there is an increased discrepancy between theoretical and experimental modulus values, notably at high fiber loadings.<sup>40</sup> The 20 wt% fiber concentration composites demonstrate the best overall agreement with the calculated values in Fig. 4 and demonstrates the least amount of error present in the ultimate tensile strength as reported in Fig. S3. Furthermore, at filler loadings greater than 20 wt%, the composites were difficult to compression mold without brittle fracture, partially due to sample porosity. Given these findings, all future reported composites were pursued as hemp fiber/PP composites at a 20 wt% filler concentration. The optimum filler concentration at 20 wt% is likely due to factors such as increased water retention of the natural fibers leading to composite porosity and fiber aggregation during mixing at high fiber loadings, leading to stress concentration points.

Hemp/PP composite materials were produced at filler concentrations of 20 wt% for the three hemp fibers and HD, and the tensile properties were measured both with and without the addition of MAPP, and results are shown in Fig. 5. MAPP was incorporated as a coupling agent at 5 wt% based on previous literature.<sup>14,20,41</sup> In all cases, the addition of just the hemp filler decreased the ultimate tensile strength and increased Young's modulus in comparison to neat PP. This finding is unsurprising given the hydrophilic nature of the filler material and the hydrophobic nature of the PP matrix, resulting in a relatively poor interfacial adhesion and has previously been reported in literature.<sup>13,14</sup>

MAPP is a known coupling/compatibilization agent for natural fibers and was expected to improve the tensile strength for all hemp fiber composites. MAPP compatibilizes the HF as it has a maleic anhydride (-MA) functional group that can participate in hydrogen bonding and covalent bonding with the HF surface hydroxyl groups resulting in a bound polymer at the interface that can interact positively with the bulk matrix. Surprisingly, only the HD resulted in a significant increase in tensile strength with the addition of MAPP; for this composition, the strength of the HD composites increased by 17%, while the elastic modulus decreased by 57%, both of which were statistically significant differences given a 95% confidence level. However, the elastic modulus of the HD composite still surpassed that of neat PP. This improvement is surprising for multiple reasons: (1) the HD has the smallest length and (2) HD exhibited the lowest cellulose (glucan) content and higher xylan, lignan, and miscellaneous contents (Table 1). The expectation was that the surface would have less reactive groups to couple with the -MA and result in either no change or reduced tensile strength. The only other HF that showed an increase in tensile strength with MAPP was the SD composites, which showed an 8.5% increase in strength and 53% increase in elastic modulus and had a larger miscellaneous content as well; Fourier transform infrared spectroscopy was performed on all fiber types to gain additional insight, as seen in Fig. S4 and discussed in the SI. Addition of MAPP to the

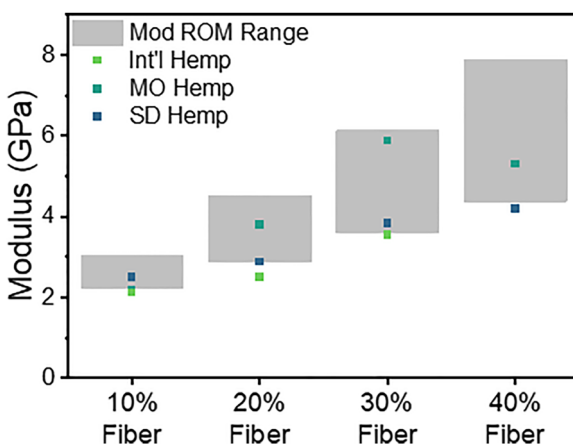


Fig. 4 A modified rule of mixtures (ROM) calculation was performed and is represented as a range of values (grey boxes), and the experimental data was compared to this calculated range with good agreement.



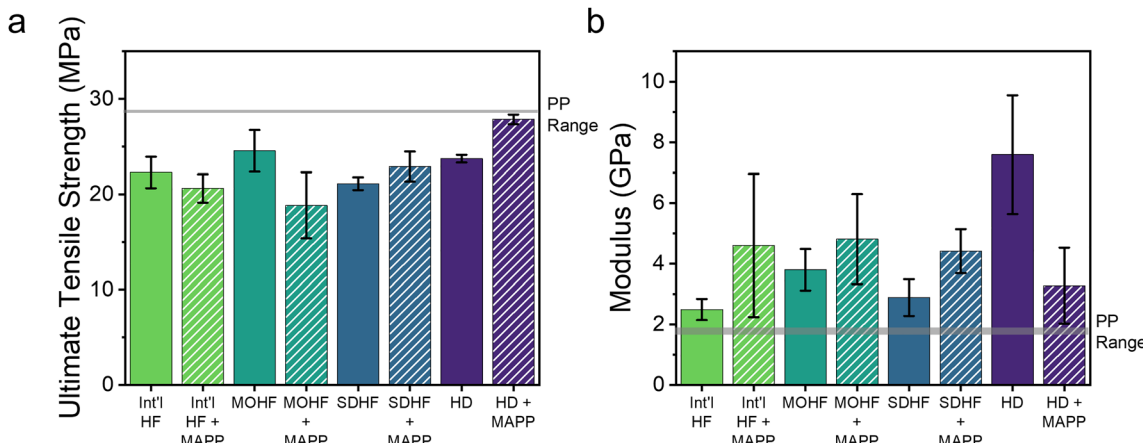


Fig. 5 Tensile results are shown as ultimate tensile strength (a) and Young's modulus (b) for all hemp/PP composites both with and without the MAPP compatibilizer present in the system.

other fiber-reinforced composites resulted in a 23% decrease in strength for the MO composites and no significant change in tensile strength for the Int'l composites. However, the elastic modulus of MO and Int'l HF also increased with the addition of MAPP by 27% and 85%, respectively. There might be multiple factors playing into the reduction of tensile strength and changes in elastic modulus for these composites; for example, differences in HF length, potential fiber alignment during compression molding, fiber dispersion and more that were not quantified for each composite type. Additional fiber treatments such as NaOH treatment and a combination of an NaOH treatment with the MAPP compatibilizer were also explored (Fig. S5), but the NaOH treatment did not provide improvements in the tensile properties as reported in prior literature for natural fibers like coir fiber<sup>42</sup> or jute.<sup>43</sup> The addition of MAPP alone was found to be the most effective and scalable compatibilization strategy.<sup>19</sup>

To investigate the potential improvement of the composites with the addition of MAPP, tensile fracture surfaces for all

composites were investigated with the use of SEM as seen in Fig. 6. White and red arrows indicate areas of poor and good filler/polymer interfacial adhesion, respectively. Qualitatively, the addition of the MAPP into the composites appears to increase interfacial adhesion for all fibers, while there is little change to the interfacial adhesion for the HD composites. This high interfacial adhesion for the HD composites without MAPP reasonably explains its excellent stiffness performance, while the increase in interfacial adhesion with MAPP inclusion for the fiber composites is reflected in the increase in stiffness as seen in Fig. 5b; this will also be discussed in a later section. In addition to fracture surfaces, optical microscopy was used to investigate the dispersion of the fillers with and without the addition of MAP, as seen in Fig. S6 and discussed in detail in the SI.

In addition to mechanical performance, a material's HDT is an important consideration in material design for automotive applications. As shown in Fig. 7a the HDT of all composite

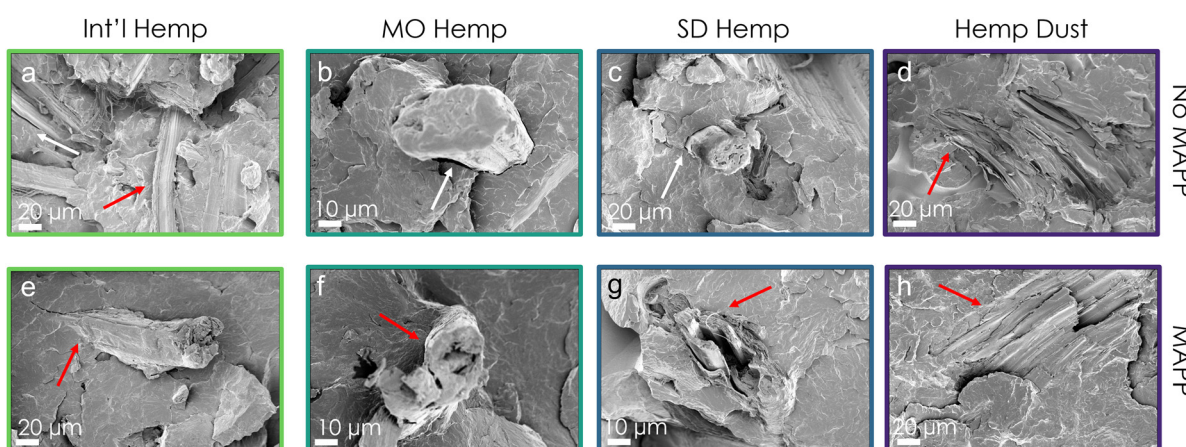


Fig. 6 SEM of the tensile fracture surfaces are shown for all composites without (a)–(d) and with (e)–(h) MAPP incorporation. Red arrows indicate areas of good interfacial adhesion between the filler and polymer interface while white arrows indicate areas of poor interfacial adhesion between the filler and polymer interface.



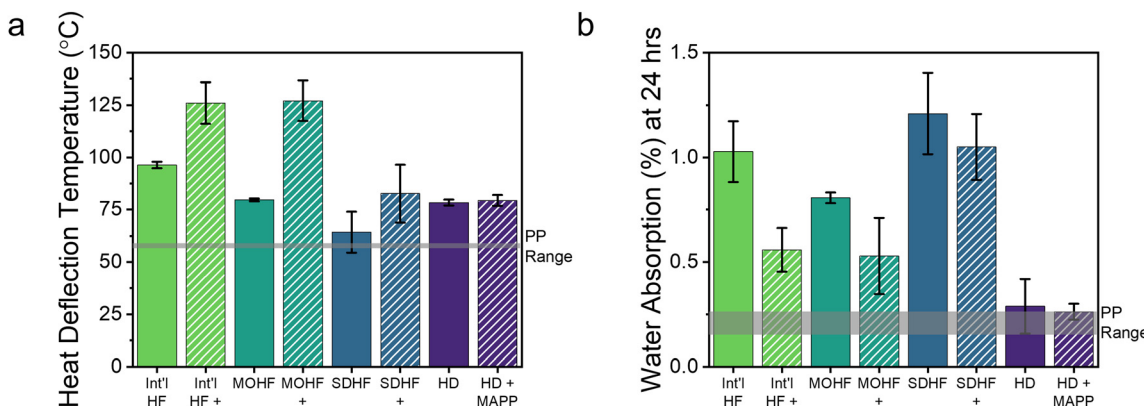


Fig. 7 All composite formulations are compared to neat PP for (a) heat deflection temperature (HDT) and (b) water absorption at 24 hours.

samples exceeded that of neat PP, and the addition of MAPP produced significant increases in HDT of 31%, 60%, and 29% for the Int'l, MO, and SD hemp composites, respectively, compared to their unmodified counterparts. The difference in HDT here cannot be attributed to crystallinity or density differences between fiber types as composites achieved similar values for both (Fig. 3) but could potentially be due to differences in length and fiber entanglement. For example, all fiber types had similar diameters, however the HD had the lowest length compared to the prepared hemp fibers which were  $\sim 6$  mm long. Moreover, the addition of MAPP to the fiber-filled composites improved the material stiffness under tension at room temperature (Fig. 5b) where this increase in stiffness also suggests an improvement in stiffness across a wider temperature range, as evidenced by the increased HDT values.

Another key consideration for automotive material feedstocks is their potential to absorb water, which can cause matrix cracking or delamination between polymer matrices and fillers and lead to early failure. For example, if the material is intended for an exterior part where it will be exposed to rain or if the vehicle is in a particularly humid climate, the water absorption of the composite can lead to early material degradation. All fiber composites produced a significantly higher water uptake after 24 hours when compared to neat PP, while the HD composites yielded a comparable water uptake to neat PP (Fig. 7b). However, the addition of MAPP into the composites yielded a reduction in water uptake up to 46%. Comparable data sets are reported for hemp/PP composites of varying fiber concentration in Fig. S7, where the chosen 20 wt% fiber concentration is validated as it minimizes composite water uptake and density. Considering the thermomechanical data, it is clear that no one hemp fiber/filler source was clearly superior to the others, which could indicate that the variability in natural fibers from different sources could be acceptable for industrial applications.

### Industrial relevance

The properties of the composites and neat PP with MAPP were then compared to those of PP with 20 wt% talc, a common

composite used in nonstructural automotive applications (Fig. 8).<sup>33,44</sup> An ideal composite formulation would decrease water absorption and density while simultaneously increasing tensile strength, modulus, and HDT. One or more of the composites produced in this study were shown to meet or exceed the PP/talc comparison in each of the parameters shown except water absorption, attributable to the highly hydrophilic nature of natural fibers in comparison to PP and talc. Additional testing to include fiber coatings should be explored moving forward to minimize the water absorption of the natural fillers. Given the competitive performance metrics of the formulated composites presented here, it is reasonable to assume that US-sourced hemp fibers are a promising composite reinforcement option for the automotive industry.

To demonstrate the scalability of these formulations and the MAPP compatibilizer that was implemented, the small-scale composites were produced *via* twin-screw extrusion as seen in Fig. S8. Essentially, the composites which were originally produced in 40–50 g batches were now melt compounded into a continuous twin-screw extruder which produced  $\sim 9$  kg of

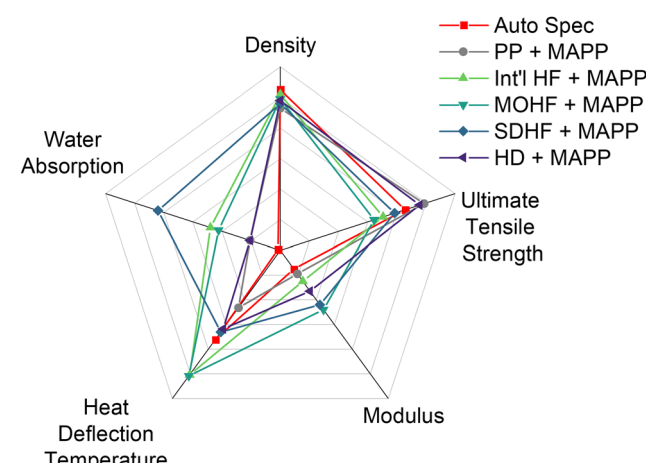


Fig. 8 A spider plot is shown comparing the materials in this study to both neat PP (grey) and an automotive industrial standard sourced from literature (PP with a 20 wt% talc fill – red).



material whose composition was PP + 20 wt% HD + 5 wt% MAPP. This composite was then injection molded into a coin-like shape, as seen in Fig. S9, to demonstrate the ability of this composite to be reasonably produced *via* conventional manufacturing techniques.

### Environmental assessment of hemp fiber transportation

Generally, LCA data is presented in a range of either a “high” or “low” value, as seen in Fig. 9, with the ideal materials displaying the lowest possible GWP and CED value. The TN sourced fibers exhibit the lowest values among all cases. Compared to the international scenario, the TN scenario shows decreased values ranging from 61–64% for GWP and 61–63% for CED. However, the most surprising results are that SD sourced fibers are somewhat comparable to internationally sourced fibers, meaning that domestically sourced fibers are not inherently the favorable option from a GWP or CED perspective. The SD fibers were transported 2245 km, which is significantly lower than the 7756 km distance travelled by France sourced fibers. While this finding may seem counterintuitive, all domestically sourced fibers were assumed to be transported exclusively *via* truck while the internationally sourced fibers were transported by truck where possible but 73% of the total distance travelled was *via* freight ship (*i.e.*, across the ocean). This is significant because for freight ocean shipping the GWP and CED is 2 orders of magnitude and 1–2 orders of magnitude lower than that of truck transportation, respectively. This signifies that to have the most favorable transportation for hemp fiber composite production, there is some maximum distance the fibers should be transported to best the international sourcing. However, the France sourced fiber is the least favorable fiber source of all considered cases. To ensure consistency, the largest volume port is considered as the shipping route for both France and the US, which is the most cost-effective option. Looking ahead, it would be beneficial to explore whether the maximum domestic transportation distance can be expanded if transportation methods such as railway (train) or air (plane) were considered,

and how these scenarios would compare to international sources of greater distance.

## Conclusions

In 2023 alone, an estimated 15.8 million automobiles were produced in North America, and approximately 10 wt% of each vehicle comprises polymers and polymer composites. Furthermore, plastic and plastic composite usage is expected to grow with the increase in electric vehicle demand, and estimates have predicted a mid-size vehicle to contain ~45% more plastics and composites compared to their internal combustion engine counterparts.<sup>1</sup> This increase in vehicle plastic usage is largely due to the need to offset electric vehicle battery weight with the use of high strength-to-weight ratio plastics to maintain reasonable fuel efficiency. As such, it is critical to understand how bio-based polymer composites can provide a sustainable substitute to purely synthetic polymer composites. In this study, two US-sourced hemp fibers, one international-sourced hemp fiber, and a hemp dust (*i.e.*, waste byproduct) were used as a reinforcing filler in PP. The incorporation of 20 wt% hemp filler yielded composites with an up to a 367% increase in Young's modulus, 126% increase in heat deflection temperature, and comparable water uptake performance. The hemp-reinforced composite properties were compared to that of a common automotive PP composite, with formulations meeting or exceeding numerous performance metrics. Results ultimately indicated that a variety of hemp sources could be viable for implementation in polymer composites for automotive applications, and additional research could explore improving the interfacial adhesion of the fiber/matrix interface, decreasing composite water absorption, and exploring other performance metrics of interest for specific part requirements. Finally, a screening analysis on hemp fiber transportation demonstrated that regionalized transportation can result in a 60.9% lower CED and a 61.4% lower GWP value when compared to requirements for those fibers shipped long distances

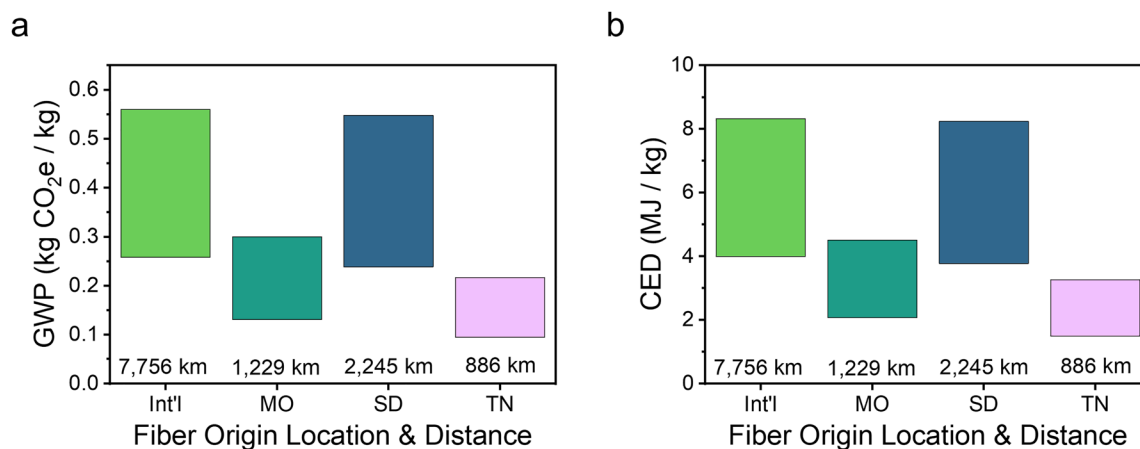


Fig. 9 Global warming potential (GWP) and cumulative energy demand (CED) is reported as a range for transportation of natural fibers from an international location (Int'l) in comparison to Missouri (MO), South Dakota (SD), and Tennessee (TN).



over land or from overseas. It was shown that both the shipping distance and mode of transportation are crucial in determining the environmental impact of a given feedstock. This study has ultimately demonstrated that hemp is a promising material for more sustainable polymer composites, particularly considering automotive applications, and while hemp from different sources does not strongly affect the composite performance, its source and transportation to the final manufacturing location must be considered for the material to remain a sustainable choice.

## Author contributions

Amber M Hubbard – conceptualization, investigation, methodology, formal analysis, funding acquisition, writing – original draft, writing – review and editing. Julia Gelfond – investigation, visualization, formal analysis, writing – review and editing. Kathryn Slavny – investigation, formal analysis, writing – review and editing. Komal Kooduvalli – formal analysis, writing – original draft, writing – review and editing. Katie Copenhaver – conceptualization, investigation, writing – review and editing. Meghan E Lamm – conceptualization, investigation, writing – review and editing. Sanjita Wasti – investigation, methodology, formal analysis, writing – original draft, writing – review and editing. Matthew Korey – formal analysis, writing – review and editing. Yunqiao Pu – investigation, writing – review and editing. Caitlyn Clarkson – writing – review and editing, formal analysis. Umesh Marathe – investigation, writing – review and editing.

## Conflicts of interest

There are no conflicts of interest to declare.

## Data availability

We note here that the majority of the data collected throughout this work are available in either the manuscript or supplemental Information (SI). See DOI: <https://doi.org/10.1039/d5ma00798d>.

Additional data may be made available upon request to the corresponding author.

## Acknowledgements

This research was supported by the U.S. Department of Energy (DOE), Advanced Manufacturing Office and used resources at the Manufacturing Demonstration Facility at Oak Ridge National Laboratory, a User Facility of DOE's Office of Energy Efficiency and Renewable Energy. This manuscript has been authored by UT-Battelle, LLC under Contract No. DE-AC05-00OR22725 with the U.S. Department of Energy. The United States Government retains and the publisher, by accepting the article for publication, acknowledges that the United States Government retains a non-exclusive, paid-up, irrevocable,

world-wide license to publish or reproduce the published form of this manuscript, or allow others to do so, for United States Government purposes. The Department of Energy will provide public access to these results of federally sponsored research in accordance with the DOE Public Access Plan (<https://energy.gov/downloads/doe-public-access-plan>). Microscopy studies were completed at the Center for Nanophase Materials Sciences, a DOE Office of Science User Facility. This work was supported in part by the U.S. Department of Energy, Office of Science, Office of Workforce Development for Teachers and Scientists (WDTD) under the Science Undergraduate Laboratory Internships Program (SULI) administered by the Oak Ridge Institute for Science and Education. This research was supported in part by an appointment to the Oak Ridge National Laboratory GRO Program, sponsored by the U.S. Department of Energy and administered by the Oak Ridge Institute for Science and Education. The authors would like to thank the Hemp Alliance of Tennessee, Ken Meyer (Complete Hemp Processing), John Peterson (Dakota Hemp), and Corbett Miteff for their collaboration and engaging discussions around hemp fiber growing and processing. The authors would also like to thank the MiniFIBERS, Inc. team, specifically Jacob Ragland and Scott Frasca, for their guidance in natural fibers and support of the project.

## References

- 1 Chemistry and Automobiles Driving the Future; 2024. <https://plasticmakers.org/wp-content/uploads/2023/02/Chemistry-and-Automobiles-2024.pdf>.
- 2 M. Carlier, Number of Vehicles in Operation in the United States Between 1st Quarter 2018 and 2nd Quarter 2024. Statista, 2024. <https://www.statista.com/statistics/859950/vehicles-in-operation-by-quarter-united-states/> (accessed 2025 April 21).
- 3 M. Carlier, Number of Motor Vehicles Registered in the United States from 1990 to 2022. Statista, 2024. <https://www.statista.com/statistics/183505/number-of-vehicles-in-the-united-states-since-1990/#:~:text=Some%20283.4%20million%20vehicles%20were,10.9%20million%20units%20in%202022> (accessed 2025 April 21).
- 4 *Lightweight Materials for Cars and Trucks*. Department of Energy Vehicle Technologies Office, 2025. <https://www.energy.gov/eere/vehicles/lightweight-materials-cars-and-trucks#:~:text=Because%20it%20takes%20less%20energy,%25%2D8%25%20fuel%20economy%20improvement> (accessed 2025 April 21).
- 5 J. Mariz, C. Guise, T. L. Silva, L. Rodrigues and C. J. Silva, Hemp: From Field to Fiber—A Review, *Textiles*, 2024, 4(2), 165–182.
- 6 A. Shahzad, Hemp fiber and its composites – a review, *J. Compos. Mater.*, 2012, 46(8), 973–986, DOI: [10.1177/0021998311413623](https://doi.org/10.1177/0021998311413623).
- 7 G. Crini, E. Lichtfouse, G. Chanet and N. Morin-Crini, Applications of hemp in textiles, paper industry, insulation



and building materials, horticulture, animal nutrition, food and beverages, nutraceuticals, cosmetics and hygiene, medicine, agrochemistry, energy production and environment: a review, *Environ. Chem. Lett.*, 2020, **18**(5), 1451–1476, DOI: [10.1007/s10311-020-01029-2](https://doi.org/10.1007/s10311-020-01029-2).

8 A. T. M. F. Ahmed, M. Z. Islam, M. S. Mahmud, M. E. Sarker and M. R. Islam, Hemp as a potential raw material toward a sustainable world: a review, *Helijon*, 2022, **8**(1), e08753, DOI: [10.1016/j.helijon.2022.e08753](https://doi.org/10.1016/j.helijon.2022.e08753).

9 *Hemptecture: Truly Sustainable Materials*. Hemptecture, 2025. <https://www.hemptecture.com/?srsltid=AfmBOoqAhmeDf95-1voDdztKvHrAhRyHWf4Kw3r5QdlQHXck4cV8XKau> (accessed 2025 April 22).

10 Z. Li, X. Wang and L. Wang, Properties of hemp fibre reinforced concrete composites, *Composites, Part A*, 2006, **37**(3), 497–505, DOI: [10.1016/j.compositesa.2005.01.032](https://doi.org/10.1016/j.compositesa.2005.01.032).

11 D. Sedan, C. Pagnoux, A. Smith and T. Chotard, Mechanical properties of hemp fibre reinforced cement: influence of the fibre/matrix interaction, *J. Eur. Ceram. Soc.*, 2008, **28**(1), 183–192, DOI: [10.1016/j.jeurceramsoc.2007.05.019](https://doi.org/10.1016/j.jeurceramsoc.2007.05.019).

12 MiniFIBERS, Inc. Technical Data Sheet Natural Fibers. MiniFIBERS, I., ed, 2024.

13 L. Stelea, I. Filip, G. Lisa, M. Ichim, M. Drobota, C. Sava and A. Muresan, Characterisation of Hemp Fibres Reinforced Composites Using Thermoplastic Polymers as Matrices, *Polymers*, 2022, **14**(3), 481, DOI: [10.3390/polym14030481](https://doi.org/10.3390/polym14030481).

14 A. Etaati, S. Pather, Z. Fang and H. Wang, The study of fibre/matrix bond strength in short hemp polypropylene composites from dynamic mechanical analysis, *Composites, Part B*, 2014, **62**, 19–28, DOI: [10.1016/j.compositesb.2014.02.011](https://doi.org/10.1016/j.compositesb.2014.02.011).

15 E. Xanthopoulou, N. Pardalis, A. Zamboulis and D. N. Bikiaris, Exploring the effect of hemp fibers' addition on the properties of PLA/PPAD biodegradable blends, *Sustainable Chem. Environ.*, 2024, **8**, 100176, DOI: [10.1016/j.scenv.2024.100176](https://doi.org/10.1016/j.scenv.2024.100176).

16 J. Arnold and D. A. Smith, 3D printed polylactic acid – hemp fiber composites: mechanical, thermal, and microcomputed tomography data, *Data Brief*, 2021, **39**, 107534, DOI: [10.1016/j.dib.2021.107534](https://doi.org/10.1016/j.dib.2021.107534).

17 G. Caprino, L. Carrino, M. Durante, A. Langella and V. Lopresto, Low impact behaviour of hemp fibre reinforced epoxy composites, *Compos. Struct.*, 2015, **133**, 892–901, DOI: [10.1016/j.compstruct.2015.08.029](https://doi.org/10.1016/j.compstruct.2015.08.029).

18 S. Panthapulakkal and M. Sain, Injection-molded short hemp fiber/glass fiber-reinforced polypropylene hybrid composites—Mechanical, water absorption and thermal properties, *J. Appl. Polym. Sci.*, 2007, **103**(4), 2432–2441, DOI: [10.1002/app.25486](https://doi.org/10.1002/app.25486).

19 R. Sepe, F. Bollino, L. Boccarusso and F. Caputo, Influence of chemical treatments on mechanical properties of hemp fiber reinforced composites, *Composites, Part B*, 2018, **133**, 210–217, DOI: [10.1016/j.compositesb.2017.09.030](https://doi.org/10.1016/j.compositesb.2017.09.030).

20 K. L. Pickering, G. W. Beckermann, S. N. Alam and N. J. Foreman, Optimising industrial hemp fibre for composites, *Composites, Part A*, 2007, **38**(2), 461–468, DOI: [10.1016/j.compositesa.2006.02.020](https://doi.org/10.1016/j.compositesa.2006.02.020).

21 C. A. Fuentes, P. Willekens, J. Petit, C. Thouminot, J. Müsing, L. M. Trindade and A. W. Van Vuure, Effect of the middle lamella biochemical composition on the non-linear behaviour of technical fibres of hemp under tensile loading using strain mapping, *Composites, Part A*, 2017, **101**, 529–542, DOI: [10.1016/j.compositesa.2017.07.017](https://doi.org/10.1016/j.compositesa.2017.07.017).

22 S. Wasti, A. M. Hubbard, C. M. Clarkson, E. Johnston, H. Tekinalp, S. Ozcan and U. Vaidya, Long Coir and Glass Fiber Reinforced Polypropylene Hybrid Composites Prepared via Wet-laid Technique, *Compos., Part C: Open Access*, 2024, 100445.

23 X. Meng, Q. Sun, M. Kosa, F. Huang, Y. Pu and A. J. Ragauskas, Physicochemical Structural Changes of Poplar and Switchgrass during Biomass Pretreatment and Enzymatic Hydrolysis, *ACS Sustainable Chem. Eng.*, 2016, **4**(9), 4563–4572, DOI: [10.1021/acssuschemeng.6b00603](https://doi.org/10.1021/acssuschemeng.6b00603).

24 J. Bare, TRACI 2.0: the tool for the reduction and assessment of chemical and other environmental impacts 2.0, *Clean Technol. Environ. Policy*, 2011, **13**(5), 687–696, DOI: [10.1007/s10098-010-0338-9](https://doi.org/10.1007/s10098-010-0338-9).

25 R. Hischier, B. Weidema, H.-J. Althaus, C. Bauer, G. Doka, R. Dones, R. Frischknecht, S. Hellweg, S. Humbert and N. Jungbluth, *Implementation of Life Cycle Impact Assessment Methods*. ecoinvent report No. 3, v2.2, 2010.

26 E. M. Ruiz, L. Valsasina, D. FitzGerald, F. Brunner, C. Vadenbo, C. Bauer, G. Bourgault, A. Symeonidis and G. Wernet, *Documentation of Changes Implemented in Ecoinvent Database V3.3*. Ecoinvent, Zurich, Switzerland, 2016.

27 G. Wernet, C. Bauer, B. Steubing, J. Reinhard, E. Moreno-Ruiz and B. Weidema, The Ecoinvent Database V3 (Part 1): Overview and Methodology, *Int. J. Life Cycle Assess.*, 2016, **21**, 1218–1230.

28 LCA Software for Informed Changemakers (SimaPro). Sustainability, P., Ed.; 2025.

29 M. Carus and L. Sarmento, The European Hemp Industry: Cultivation, Processing, and Applications for Fibres, Shives, Seeds and Flowers, *Eur. Ind. Hemp Assoc.*, 2016, **5**, 1–9.

30 P. P. A. A. H. Kandelaars and J. D. v Dam, An analysis of variables influencing the material composition of automobiles, *Resour. Conserv. Recycl.*, 1998, **24**(3–4), 323–333, DOI: [10.1016/S0921-3449\(98\)00061-5](https://doi.org/10.1016/S0921-3449(98)00061-5).

31 R. Conrad, Automotive Polymers. Kuraray Elastomer, 2024. <https://www.elastomer.kuraray.com> (accessed 2024 March 28).

32 *Polymers*. British Plastics Federation, 2025. <https://www.bpf.co.uk/> (accessed 2025 April 21).

33 S. Baily and R. Davey, Polypropylene – PP 20% Talc Filled, *Azo Mater.*, 2022, <https://www.azom.com/article.aspx?ArticleID=829> (accessed 2025 April 21).

34 V. Kholodovych and W. J. Welsh, Densities of Amorphous and Crystalline Polymers, in *Physical Properties of Polymers Handbook*, ed. J. E. Mark, Springer, New York, 2007, pp. 611–617.

35 J. Agarwal, S. Mohanty and S. K. Nayak, Influence of cellulose nanocrystal/sisal fiber on the mechanical, thermal, and morphological performance of polypropylene hybrid composites, *Polym. Bull.*, 2021, **78**, 1609–1635, DOI: [10.1007/s00289-020-03178-4](https://doi.org/10.1007/s00289-020-03178-4).



36 P. da Silveira, M. Santos, Y. S. Chaves, M. P. Ribeiro, B. Z. Marchi, S. N. Monteiro, A. V. Gomes, N. C. O. Tapanes, P. Pereira and D. C. Bastos, Characterization of Thermo-Mechanical and Chemical Properties of Polypropylene/Hemp Fiber Biocomposites: Impact of Maleic Anhydride Compatibilizer and Fiber Content, *Polymers*, 2023, **15**(15), 3271, DOI: [10.3390/polym15153271](https://doi.org/10.3390/polym15153271).

37 L. Wang, W. Gramlich, D. Gardner, Y. Han and M. Tajvidi, Spray-Dried Cellulose Nanofibril-Reinforced Polypropylene Composites for Extrusion-Based Additive Manufacturing: Nonisothermal Crystallization Kinetics and Thermal Expansion, *J. Compos. Sci.*, 2018, **2**(1), 7, DOI: [10.3390/jcs2010007](https://doi.org/10.3390/jcs2010007).

38 C. W. Huang, T. C. Yang, K. C. Hung, J. W. Xu and J. H. Wu, The Effect of Maleated Polypropylene on the Non-Isothermal Crystallization Kinetics of Wood Fiber-Reinforced Polypropylene Composites, *Polymers*, 2018, **10**(4), 382, DOI: [10.3390/polym10040382](https://doi.org/10.3390/polym10040382).

39 F. Meng, E. A. Olivetti, Y. Zhao, J. C. Chang, S. J. Pickering and J. McKechnie, Comparing Life Cycle Energy and Global Warming Potential of Carbon Fiber Composite Recycling Technologies and Waste Management Options, *ACS Sustainable Chem. Eng.*, 2018, **6**(8), 9854–9865, DOI: [10.1021/acssuschemeng.8b01026](https://doi.org/10.1021/acssuschemeng.8b01026).

40 Z. Luo, X. Li, J. Shang, H. Zhu and D. Fang, Modified rule of mixtures and Halpin–Tsai model for prediction of tensile strength of micron-sized reinforced composites and Young's modulus of multiscale reinforced composites for direct extrusion fabrication, *Adv. Mech. Eng.*, 2018, **10**(7), 1687814018785286, DOI: [10.1177/1687814018785286](https://doi.org/10.1177/1687814018785286).

41 P. Mutjé, A. Lòpez, M. E. Vallejos, J. P. López and F. Vilaseca, Full exploitation of Cannabis sativa as reinforcement/filler of thermoplastic composite materials, *Composites, Part A*, 2007, **38**(2), 369–377, DOI: [10.1016/j.compositesa.2006.03.009](https://doi.org/10.1016/j.compositesa.2006.03.009).

42 S. Wasti, F. Vautard, C. Clarkson, S. Bhagia, H. M. Meyer, A. Gosnell, H. Tekinalp, S. Ozcan and U. Vaidya, Effects of mercerization and fiber sizing of coir fiber for utilization in polypropylene composites, *Cellulose*, 2024, **31**(10), 6317–6334, DOI: [10.1007/s10570-024-05997-4](https://doi.org/10.1007/s10570-024-05997-4).

43 J. A. Khan, M. A. Khan and R. Islam, Effect of mercerization on mechanical, thermal and degradation characteristics of jute fabric-reinforced polypropylene composites, *Fibers Polym.*, 2012, **13**(10), 1300–1309, DOI: [10.1007/s12221-012-1300-8](https://doi.org/10.1007/s12221-012-1300-8).

44 *Material Property Data*. Matweb, 2025. <https://www.matweb.com/search/PropertySearch.aspx> (accessed 2025 April 21).

